Title	Influence of stagnant zones on transient and asymptotic dispersion in macroscopically homogeneous porous media.
Author(s)	Kandhai, D.; Hlushkou, D.; Hoekstra, Alfons G.; Sloot, Peter M. A.; Van As, H.; Tallarek, U.
Citation	Kandhai, D., Hlushkou, D., Hoekstra, A. G., Sloot, P. M. A., Van As, H., & Tallarek, U. (2002). Influence of Stagnant Zones on Transient and Asymptotic Dispersion in Macroscopically Homogeneous Porous Media. Physical Review Letters, 88(23).
Date	2002
URL	http://hdl.handle.net/10220/10187
Rights	© 2002 The American Physical Society. This paper was published in Physical Review Letters and is made available as an electronic reprint (preprint) with permission of The American Physical Society. The paper can be found at the following official DOI: [http://dx.doi.org/10.1103/PhysRevLett.88.234501]. One print or electronic copy may be made for personal use only. Systematic or multiple reproduction, distribution to multiple locations via electronic or other means, duplication of any material in this paper for a fee or for commercial purposes, or modification of the content of the paper is prohibited and is subject to penalties under law.

Influence of Stagnant Zones on Transient and Asymptotic Dispersion in Macroscopically Homogeneous Porous Media

D. Kandhai,[1,2] D. Hlushkou,[3,4] A. G. Hoekstra,[1] P. M. A. Sloot,[1] H. Van As,[5] and U. Tallarek[5,6,*]

[1]*Section Computational Science, Faculty of Science, University of Amsterdam, Kruislaan 403 1098 SJ Amsterdam, The Netherlands*

[2]*Kramers Laboratorium voor Fysische Technologie, Faculty of Applied Sciences, Delft University of Technology, Prins Bernhardlaan 6, 2628 BW Delft, The Netherlands*

[3]*Max Planck Institute for the Dynamics of Complex Technical Systems, Sandtorstrasse 1, 39106 Magdeburg, Germany*

[4]*Department of System Analysis, Belarusian State University, 4, Francisk Scoryna Avenue, Minsk, 220050, Belarus*

[5]*Laboratory of Molecular Physics and Wageningen NMR Centre, Wageningen University, Dreijenlaan 3, 6703 HA Wageningen, The Netherlands*

[6]*Lehrstuhl für Chemische Verfahrenstechnik, Otto-von-Guericke Universität Magdeburg, Universitätsplatz 2, 39106 Magdeburg, Germany*

(Received 27 November 2001; published 24 May 2002)

The role of stagnant zones in hydrodynamic dispersion is studied for creeping flow through a fixed bed of spherical permeable particles, covering several orders of characteristic time and length scales associated with fluid transport. Numerical simulations employ a hierarchical model to cope with the different temporal and spatial scales, showing good agreement with our experimental results on diffusion-limited mass transfer, transient, and asymptotic longitudinal dispersion. These data demonstrate that intraparticle liquid holdup in macroscopically homogeneous porous media clearly dominates over contributions caused by the intrinsic flow field heterogeneity and boundary-layer mass transfer.

DOI: 10.1103/PhysRevLett.88.234501 PACS numbers: 47.15.Gf, 05.60.–k, 47.55.Mh

A detailed understanding of transport in porous media over the intrinsic temporal and spatial scales is important in many technological and environmental processes [1]. For example, natural and industrial materials such as soil, rock, filter cakes, or catalyst pellets often contain low-permeability zones with respect to hydraulic flow of liquid through the medium or even stagnant regions which then remain purely diffusive. The relevance of stagnant zones stems from their influence on dispersion: Fluid molecules entrained in the deep diffusive pools cause a substantial holdup contribution and thereby affect the time scale of transient dispersion, as well as the value of the asymptotic dispersion coefficient (if the asymptotic long-time limit can be reached at all) [2–4]. Consequently, the associated kinetics of mass transfer between fluid percolating through the medium and stagnant fluid becomes rate limiting in a number of dynamic processes, including the separation and reaction efficiency of chromatographic columns and reactors, or economic oil recovery from a reservoir.

In this respect, transport phenomena observed in model systems such as random packings of spheres may help to characterize materials with a higher disorder [5–7]. For random packings of *nonporous* (impermeable) particles, for example, the long-time longitudinal dispersion coefficient is dominated by the boundary-layer contribution (due to the no-slip condition at the solid-liquid interface) or by medium and large-scale velocity fluctuations in the flow field depending on the actual disorder of the medium and the Peclet number, $Pe = \frac{u_{av} d_p}{D_m}$ (with u_{av}, the average velocity; d_p, particle diameter; and D_m, the molecular diffusivity) [6,8]. This behavior contrasts with random packings of *porous* (permeable) particles. In that case, liquid holdup associated with stagnant zones inside the particles may dominate dispersion when convective times $t_c = \frac{u_{av} t}{d_p}$ significantly exceed the dimensionless time for diffusion, $t_d = \frac{D_m t}{d_p^2}$ [9]. In many situations, however, both a macroscopic flow heterogeneity and solute trapping in stagnant zones contribute to transient and asymptotic dispersion [3,7,9].

Despite numerous theoretical, experimental, and numerical studies (e.g., [1,7,8,10–12]), the transient and asymptotic behavior of dispersion in porous media is not completely understood [13]. In particular, the influence of stagnant zones with respect to the actual mesoscopic and macroscopic flow field heterogeneity of the medium has found little attention in theory and experiment, and furthermore, the additional length and time scale associated with transport in stagnant regions complicates numerical simulations. Therefore it leaves the controversy about the dominating contribution to dispersion and the origin of long-time tails in residence-time distributions unresolved [3,7,14], let alone the question whether hydrodynamic dispersion coefficients exist at all [13]. In this Letter, we are able to resolve this issue experimentally and numerically for a macroscopically homogeneous medium by considering transient and asymptotic dispersion in a random packing of porous spheres, i.e., in a medium with bimodal porosity and associated length scales that differ by orders of magnitude. The results are contrasted to the behavior observed in packed beds of nonporous spheres.

In the experiments we used pulsed field gradient nuclear magnetic resonance (PFG-NMR) [15] to measure over

discrete temporal and spatial domain longitudinal nuclear spin (hence, molecular) displacement probability distributions of the fluid molecules in single-phase incompressible flow through beds of porous particles with average diameter (d_p) of 50 and 34 μm packed into a 4.6 mm internal diameter (d_c) cylindrical column. Pores inside the particles have a mean diameter (d_{pore}) of only 12 nm. In this hierarchical pore network the size of interparticle voids is about 25%–40% of the particle size and exceeds the intraparticle pore size by a factor of more than 10^3. One of the consequences is that transport of solutes also occurs on separate scales and is governed by different mechanisms [7,9], i.e., while the forced convection dominates transport between particles, diffusion is the only effective mechanism—based on pore space permeability [1]—that operates inside the particles.

Mainly due to this large variety of spatial and temporal domains we did not attempt a model which simultaneously resolves the fluid dynamics on column, particle, and pore scale, but exploited a hierarchical approach in the numerical simulations: A lattice-Boltzmann (LB) algorithm [16,17] was implemented for computing the flow field in computer-generated models of the interparticle pore space, and a particle tracking method was then used to record tracer dispersion in the total interconnected pore network (between and inside particles) [12]. The influence of pore space morphology in a single particle on the effective intraparticle diffusivity (D_{intra}) is not modeled explicitly, but is lumped into the model by using D_{intra} obtained from the PFG-NMR measurements. In dealing with the geometrical restrictions for tracer flux through the spheres external surface, we followed a probabilistic approach. Close to this interface fluid transport is diffusive in the inner (D_{intra}) and outer ($D_{\text{inter}} = D_m$) pore space. Corresponding differences in diffusive displacements become apparent in different probabilities for entering (p_e) or leaving (p_l) particles and can be shown by using mass balance arguments to follow the relation

$$\frac{p_e}{p_l} = \frac{D_{\text{intra}} \times \epsilon_{\text{intra}}}{D_m}, \tag{1}$$

with ϵ_{intra} the porosity of the intraparticle pore space. In the final flow simulations a periodic packing with dimension $800 \times 200 \times 200$ (with bead particles of diameter 20 lattice points) was used, and the particle tracking calculations were performed by using 500 000 particles and a time step of $0.1h$ (with h the lattice spacing). A more detailed description of the numerical methods and generated porous media including finite-size effects can be found elsewhere [18]. It should be noted that this numerical approach involves only a single free parameter, D_{intra}.

Figure 1 compares simulated displacement probability distributions (propagators) $P_{av}(R, \Delta)$ in random packings of nonporous and porous spheres where R is the net displacement of the tracer over time Δ. Characteristic differences in propagator position and shape for the otherwise identical sphere packings originate in the existence of an intraparticle stagnant zone in the case of porous particles. While the volumetric flow rate is identical

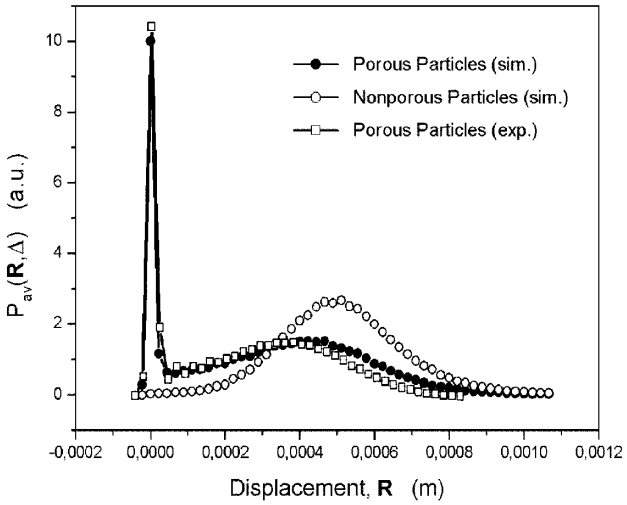

FIG. 1. Simulated and measured displacement probability distributions for liquid flow through a fixed bed of spheres after $\Delta = 25$ ms (porosity of the inter- and intraparticle pore space, $\epsilon_{\text{inter}} = 0.37$ and $\epsilon_{\text{intra}} = 0.45$, $D_{\text{intra}} = 7.3 \times 10^{-6}$ cm^2 s^{-1}, $d_p = 50$ μm, $Pe = \frac{u_{av} d_p}{D_m} = 274$ and $Re = \frac{u_{av} d_p}{\nu} = 0.66$ with kinematic viscosity: $\nu = 8.9 \times 10^{-3}$ cm^2 s^{-1}). Liquid phase: degassed water.

in both cases, it results in different averaged velocities through the bed according to the total porosity of the respective pore space. Consequently, at observation times $\Delta < \frac{r_p^2}{2D_{\text{intra}}}$ (r_p is the particle radius) we expect a stagnant, i.e., diffusion-limited fluid fraction in $P_{av}(R, \Delta)$ very close to zero net displacement containing molecules that have remained inside the particles over time Δ (diffusive ensemble). Fluid molecules leaving (or entering) the sphere gain (have gained) a net displacement due to interparticle convection. By contrast, $P_{av}(R, \Delta)$ for the random packing of nonporous spheres does not reveal diffusion-limited fluid molecules. Those which temporarily experience the no-slip condition at the solid-liquid interface exchange rapidly with downstream velocities in channels of only a few micrometers in dimension. As also seen in Fig. 1 the simulated bimodal propagator distributions obtained for porous particles are in good agreement with the results of PFG-NMR measurements. By recording the amount of stagnant fluid molecules at increasing Δ that remain unexchanged with interparticle velocities, $A_{\text{intra}}(\Delta)$, we can monitor a (fictitious) emptying of the spherical particles characterized by the classical mass transfer rate constant $B_{\text{intra}} = \pi^2 \frac{D_{\text{intra}}}{r_p^2}$ [19]

$$\frac{A_{\text{intra}}(\Delta)}{A_{\text{intra}}(0)} = \frac{6}{\pi^2} \sum_{n=1}^{\inf} \frac{1}{n^2} \exp(-n^2 B_{\text{intra}} \Delta). \tag{2}$$

Figure 2 demonstrates that the experimental and simulated intraparticle mass transfer kinetics match satisfactorily (within 3%) using $D_{\text{intra}} = 7.3 \times 10^{-6}$ cm^2 s^{-1} and $r_p = 2.5 \times 10^{-5}$ m in both cases. As mentioned, this value for D_{intra} is obtained from the experimental data ($B_{\text{intra}} = 11.52$ s^{-1}) [19] and then used in the simulations to reconstruct diffusion-limited mass transfer. The

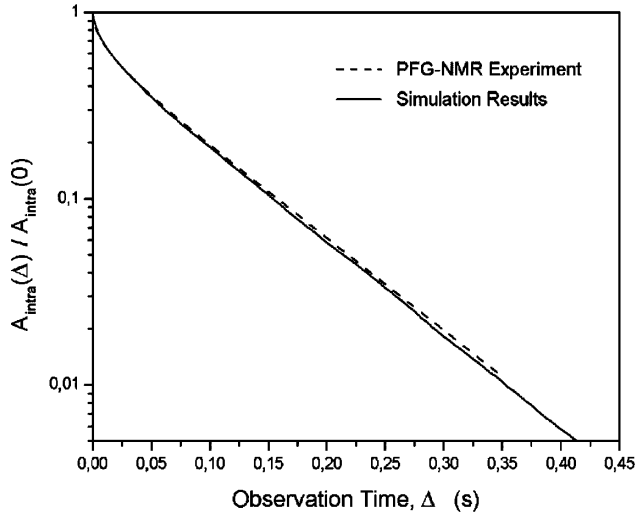

FIG. 2. Intraparticle stagnant mobile phase mass transfer kinetics ($d_p = 50\ \mu$m, $Pe = 274$).

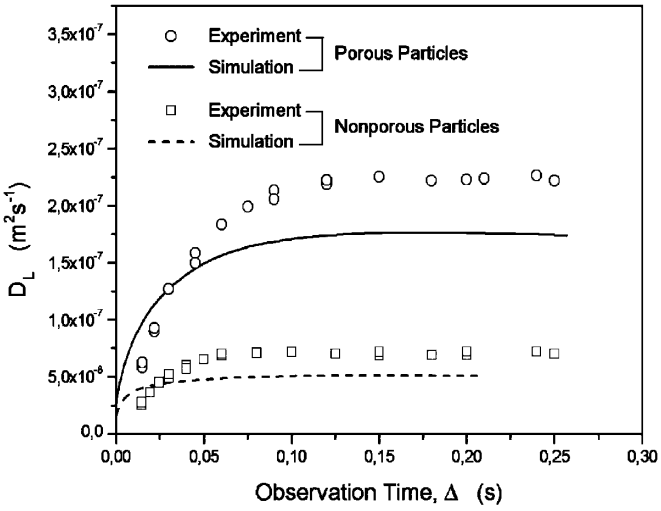

FIG. 3. Time-dependent longitudinal dispersion for flow through random packings of porous and nonporous spheres. In both cases $d_p = 34\ \mu$m, $\epsilon_{\text{inter}} = 0.37$, $Pe = 54$ and $Re = 0.13$.

results in Fig. 2 demonstrate that the semiempirical simulation procedure followed in this Letter works well, as does Eq. (2) in describing both data sets.

Thus, mass transfer in these spatially discrete stagnant zones (uniform spheres) has been adequately accounted for and allows us to focus now on its influence on longitudinal dispersion which we analyze by [12]

$$D_L(t) = \int_0^t C_L(t')\, dt', \tag{3}$$

where $C_L(t) = \sum_{i=1}^{N} [u_i(t) - u_{av}][u_i(0) - u_{av}]$ is the velocity autocovariance [N is the number of tracer particles and $u_i(t)$ is the longitudinal velocity of particle i at time t]. Figure 3 compares transient behavior at constant Pe ($d_p = 34\ \mu$m, $d_c = 4.6$ mm). In both experiment and simulation $D_L(t)$ for the nonporous particles reaches its asymptotic value (D_L^*) in a much shorter time (after approximately 50 ms) than with the porous particles (ca. 160 ms). While we observe a good agreement between simulation and experiment concerning this time scale, D_L^* itself is underestimated by the simulation in either case (by up to 25%). This effect seems to be systematic as it appears for packings of porous and nonporous particles and is probably caused by inaccuracies in the LB flow field (notice that the relative error in the hydraulic permeability, a measure of the flow resistance by the solid phase, is around 11%) [18]. Other possible explanations are related to the influence of the column wall confining the sphere packing [20], bead particles not being perfectly monodisperse (as evident from Fig. 2, cf. [19]), and the fact that the nonporous particles actually have small (micro)pores at the surface which contribute to a finite but small particle holdup. With the independently measured D_{intra} and known r_p, intraparticle diffusion can be identified as the most persistent contribution to transient dispersion in the random packing of porous spheres, i.e., the holdup dispersion mechanism reaches its long-time behavior after $t_h = \frac{r_p^2}{2D_{\text{intra}}}$ [19]. For nonporous particles, on the other hand, we find a qualitative agreement between the corresponding time scale (about 50 ms, Fig. 3) and characteristic time for boundary-layer dispersion ($t_b = 40$ ms) based on the nonlocal dispersion theory of Koch and Brady [2]. This transient behavior may be also due to mechanical dispersion [12,18]. Further work is needed to resolve these contributions in macroscopically homogeneous beds of nonporous particles.

Figure 4 compares the velocity dependence of asymptotic dispersion coefficients for random packings of porous and nonporous spheres in the range $0.1 < Pe < 100$. While the simulated data again underestimate experimental values of D_L^* (cf. Fig. 3) the effect of intraparticle liquid holdup on a significantly increased dispersion is evident. Already Aris [21] showed that this contribution scales with Pe^2, a result that was rediscovered later by Koch and Brady [8]. When analyzing the dependence of D_L^* on Pe we have to account for longitudinal diffusion, mechanical dispersion (Θ_m), boundary layer mass transfer (Θ_b) and, of course, the intraparticle holdup (Θ_h) [7,8]

$$\frac{D_L^*}{D_m} = \tau + \Theta_m Pe + \Theta_b Pe \ln(Pe) + \Theta_h Pe^2. \tag{4}$$

For $Pe \to 0$ $\frac{D_L^*}{D_m}$ approaches the packed beds tortuosity factor (τ) which represents the long-time diffusion coefficient in the interconnected pore space. This value has been measured independently by PFG-NMR (without flow) and is subsequently used in the analysis. We then fitted the experimental data, D_L^* vs Pe (Fig. 4), to Eq. (4) and the values of the parameters $(\tau, \Theta_m, \Theta_b, \Theta_h)$ thus obtained are $(0.51, 0.153 \pm 9 \times 10^{-3}, 0.080 \pm 5 \times 10^{-3}, 1.65 \times 10^{-3} \pm 2 \times 10^{-4})$ and $(0.74, 0.144 \pm 0.016, 0.101 \pm 0.011, 0.020 \pm 6 \times 10^{-4})$ for the packings of nonporous and porous spheres, respectively. The most striking feature of this analysis is the substantial difference in Θ_h characterizing holdup dispersion. Further, mechanical

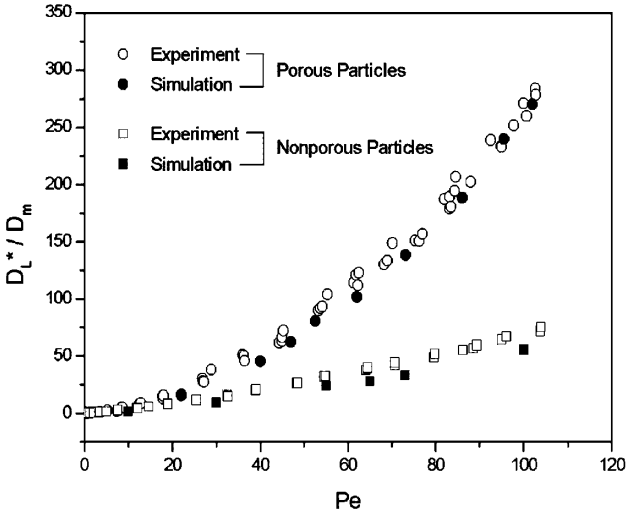

FIG. 4. Dependence of asymptotic longitudinal dispersion on Peclet number in fixed beds of porous and nonporous particles ($d_p = 34$ μm, $d_c = 4.6$ mm). Liquid phase: water. The experimental data in Figs. 3 and 4 were obtained with an accuracy of better than 5%.

dispersion is very similar in both columns which were packed and consolidated by the same procedure. Values for Θ_m (0.153 and 0.144) are actually of the same order as $\Theta_m = 0.25$ reported by Maier *et al.* [12] for their simulation of dispersion in random packings of nonporous spheres, in the range $1 < Pe < 5000$ and with $\epsilon_{\text{inter}} = 0.44$. As has already been pointed out by these authors, values for Θ_b found in our work (0.08 and 0.101), together with their own value (0.03) suggest that boundary layer dispersion is much lower than predicted by the theory of Koch and Brady [8]. A possible explanation for this discrepancy may be found in the significantly different porosities considered in that theory, on one hand, and the simulations and experiment on the other. Even the relatively small difference in particle volume fractions of the systems used by Maier *et al.* [12] ($\epsilon_{\text{inter}} = 0.44$) and in this work ($\epsilon_{\text{inter}} = 0.37$) may contribute significantly to the observed differences in Θ_m and Θ_b.

To conclude, the present work combines experimental and numerical elements to differentiate between dispersion mechanisms that originate in stagnant and flowing regions of a macroscopically homogeneous porous medium. The numerical simulations employ a semiempirical hierarchical model with a single free parameter to cope with the large variety of temporal and spatial scales. The results are in good agreement with our experimental data and clearly demonstrate the dominating contribution of liquid holdup to transient (Fig. 3) and asymptotic (Fig. 4) longitudinal dispersion in a random packing of porous spheres with column-to-particle diameter ratio above 100. Persistent effects due to flow field nonuniformities were not identified which suggests that characteristic times for mechanical dispersion are short compared to the diffusive time of this nonmechanical contribution. These findings suggest that holdup dispersion in porous media may be more important than assumed in many cases [3,7,14]. One of the remaining challenges is to characterize the relative importance of mechanical and nonmechanical dispersion mechanisms when the heterogeneity length scale is increased, e.g., in a confined random sphere packing with smaller column-to-particle diameter ratio. Then, the macroscopic flow profile may start to dominate dispersion and prevent an observation of Gaussian residence-time distributions [20,22].

*Corresponding author.
Email address: ulrich.tallarek@vst.uni-magdeburg.de

[1] J. Bear, *Dynamics of Fluids in Porous Media* (Dover, New York, 1988).
[2] D. L. Koch and J. F. Brady, Chem. Eng. Sci. **42**, 1377 (1987).
[3] J. Salles, J.-F. Thovert, R. Delannay, L. Prevors, J.-L. Auriault, and P. M. Adler, Phys. Fluids A **5**, 2348 (1993).
[4] J. P. Hulin, Adv. Colloid Interface Sci. **49**, 47 (1994).
[5] J.-C. Bacri, N. Rakotamala, and D. Salin, Phys. Rev. Lett. **58**, 2035 (1987).
[6] E. Charlaix, J. P. Hulin, and T. J. Plona, Phys. Fluids **30**, 1690 (1987).
[7] M. Sahimi, *Flow and Transport in Porous Media and Fractured Rock* (VCH, Weinheim, 1995).
[8] D. L. Koch and J. F. Brady, J. Fluid Mech. **154**, 399 (1985).
[9] J. C. Giddings, *Dynamics of Chromatography: Principles and Theory* (Marcel Dekker, New York, 1965), Part I.
[10] L. Lebon, L. Oger, J. Leblond, J. P. Hulin, N. S. Martys, and L. M. Schwartz, Phys. Fluids **8**, 293 (1996).
[11] S. Stapf, K. J. Packer, R. G. Graham, J.-F. Thovert, and P. M. Adler, Phys. Rev. E **58**, 6206 (1998).
[12] R. S. Maier, D. M. Kroll, R. S. Bernard, S. E. Howington, J. F. Peters, and H. T. Davis, Phys. Fluids **12**, 2065 (2000).
[13] C. P. Lowe and D. Frenkel, Phys. Rev. Lett. **77**, 4552 (1996).
[14] J. H. Knox, J. Chromatog. A **831**, 3 (1999).
[15] P. T. Callaghan, *Principles of Nuclear Magnetic Resonance Microscopy* (Oxford University Press, Oxford, 1993).
[16] R. Benzi, S. Succi, and M. Vergassola, Phys. Rep. **222**, 145 (1992).
[17] S. Chen and G. D. Doolen, Annu. Rev. Fluid Mech. **30**, 329 (1998).
[18] D. Kandhai, U. Tallarek, D. Hlushkou, A. G. Hoekstra, P. M. A. Sloot, and H. Van As, Philos. Trans. R. Soc. London A **360**, 521 (2002).
[19] U. Tallarek, F. J. Vergeldt, and H. Van As, J. Phys. Chem. B **103**, 7654 (1999).
[20] R. S. Maier, D. M. Kroll, R. S. Bernard, S. E. Howington, J. F. Peters, and H. T. Davis, Philos. Trans. R. Soc. London A **360**, 497 (2002).
[21] R. Aris, Chem. Eng. Sci. **11**, 194 (1959).
[22] U. Tallarek, T. W. J. Scheenen, and H. Van As, J. Phys. Chem. B **105**, 8591 (2001).